Supporting Information

Theoretical *S*tudy of Transition Metal–Doped β_{12} Borophene as New Single Atom Catalysts for Carbon Dioxide Electroreduction

Hongjie Huang[a,b#], Mingyao Chen[b#], Rongxin Zhang[b#], Yuxuan Ding[b], Hong Huang[b], Zhangfeng Shen[b], Lingchang Jiang[b], Zhigang Ge[b], Hongtao Jiang[a], Minhong Xu[c], Yangang Wang*[b] and Yongyong Cao*[b]*

[a] *Institute of Industrial Catalysis, College of Chemical Engineering, State Key Laboratory Breeding Base of Green-Chemical Synthesis Technology, Zhejiang University of Technology, Hangzhou 310032, P. R. China*

[b] *College of Biological, Chemical Science and Engineering, Jiaxing University, Jiaxing 314001, Zhejiang, P. R. China*

[c] *Department of Materials Engineering, Huzhou University, Huzhou 313000, Zhejiang, P. R. China*

*** Corresponding author:**

E-mail address: E-mail address: xumh123@163.com (M. Xu)

ygwang8136@mail.zjxu.edu.cn (Y. Wang)

cyy@zjxu.edu.cn (Y. Cao)

# These authors contributed equally to this work

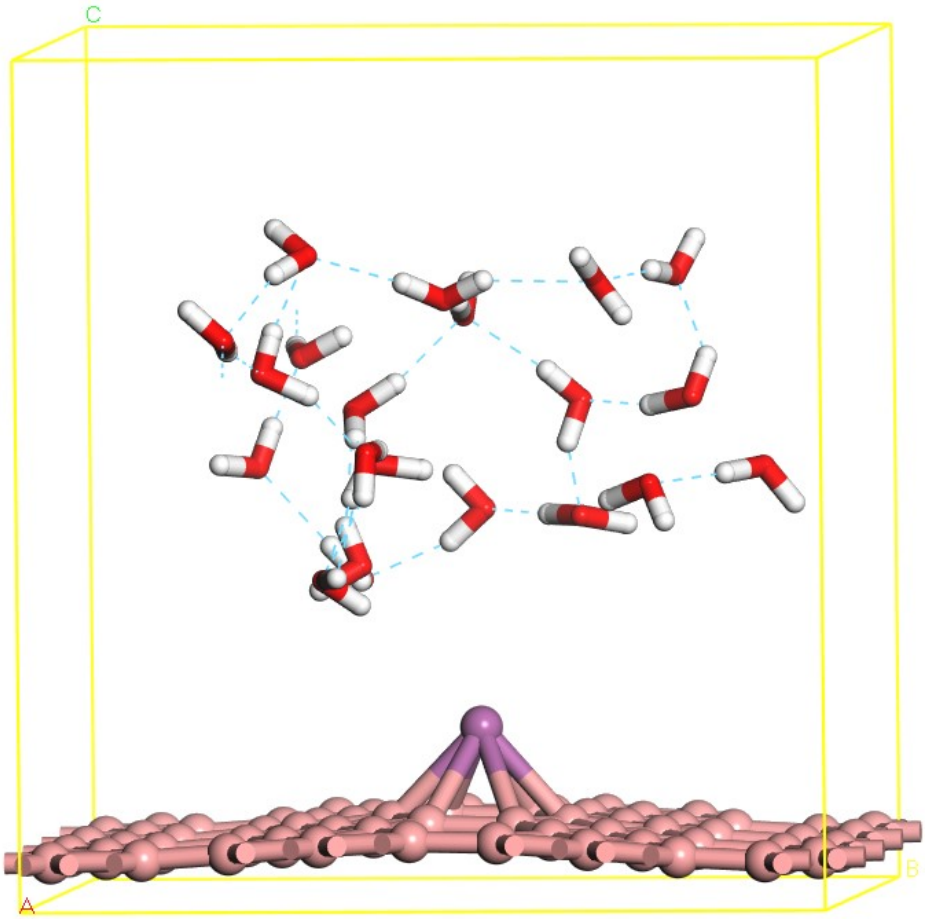

Figure S1. The model of the catalyst in the environment of 21 water molecules.

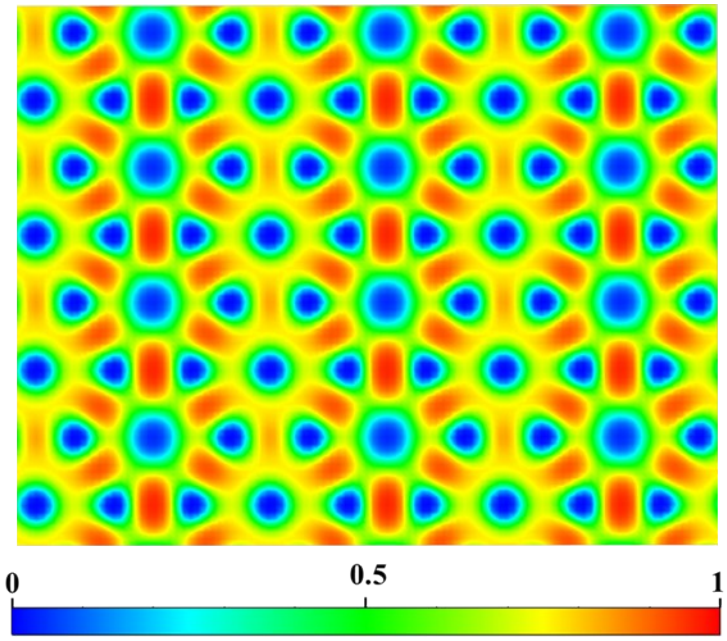

Figure S2. The electronic local function (ELF) diagrams of β_{12} borophene.

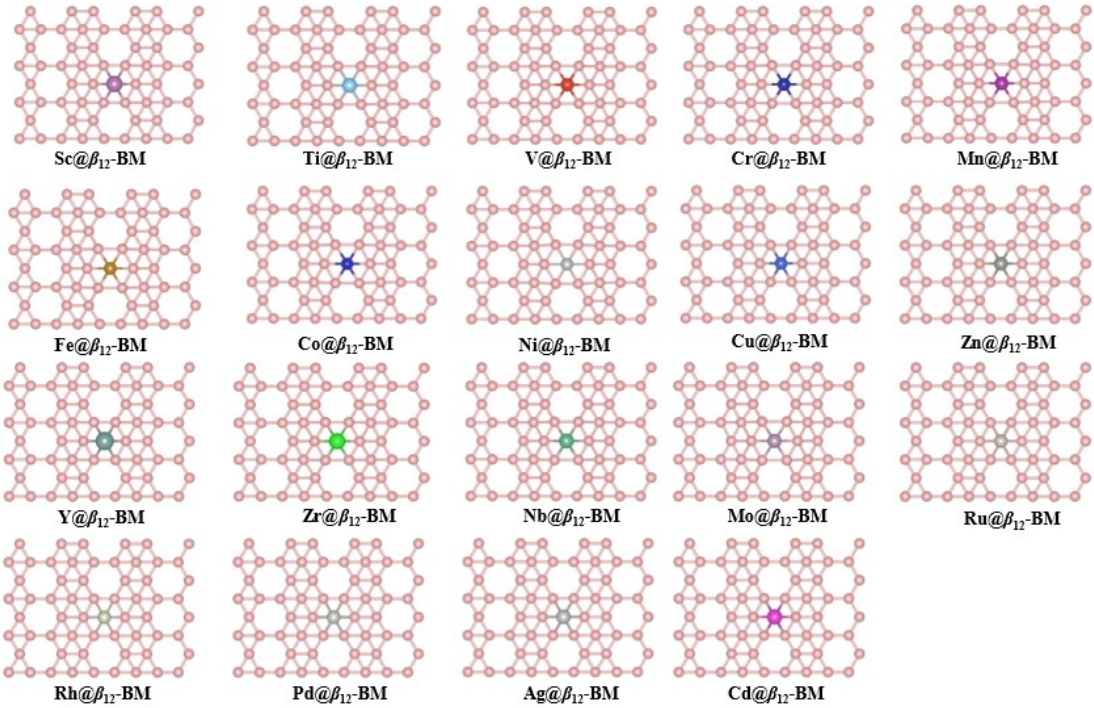

Figure S3. Optimized models of a single transition metal atom supported on β_{12}-borophene (TM@β_{12}-BM).

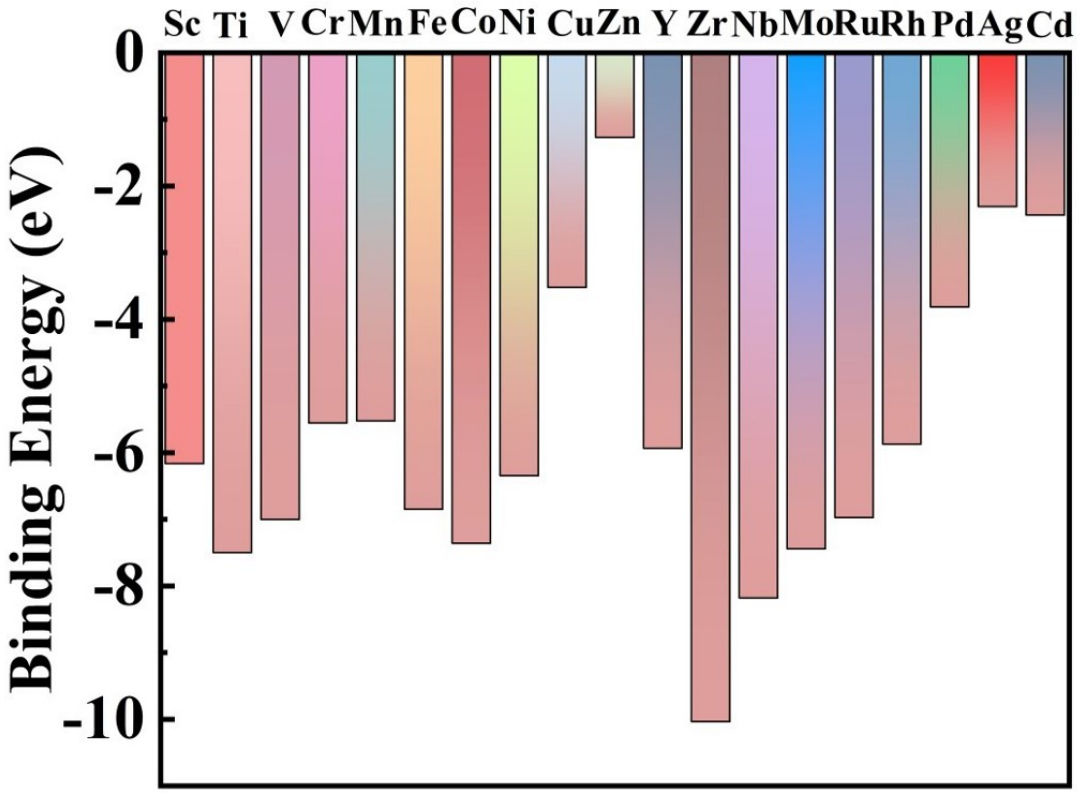

Figure S4. Binding energies of 19 catalysts (TM@β_{12}-BM).

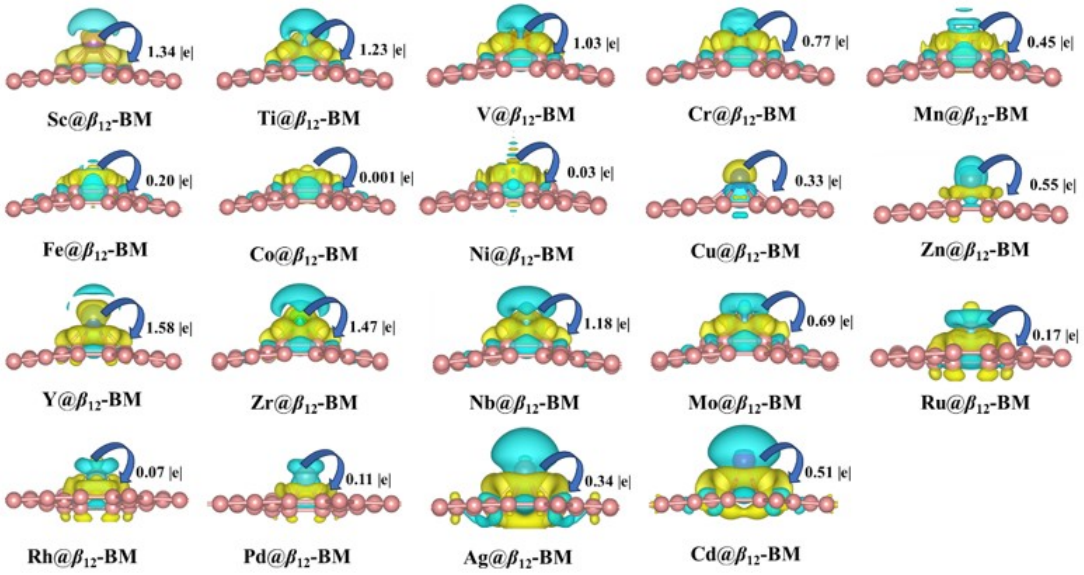

Figure S5. The charge density difference for 19 stable catalysts. The charge accumulation and depletion were depicted by yellow and green, respectively. The transferred charge from TM to β_{12}-BM is labelled as well.

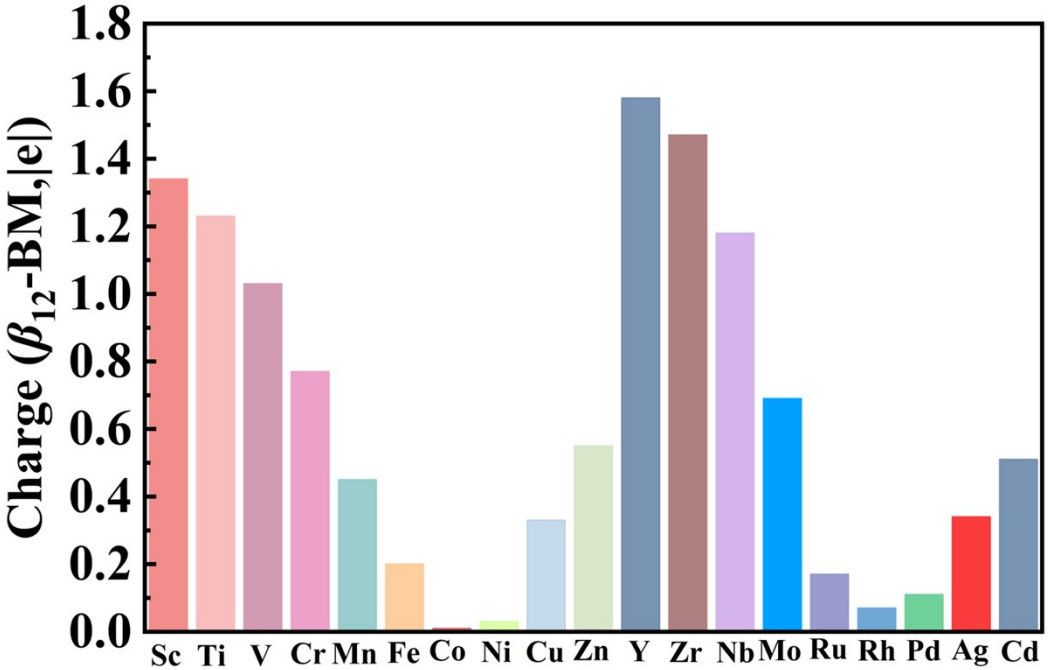

Figure S6. The transferred charge from TM to β_{12}-BM.

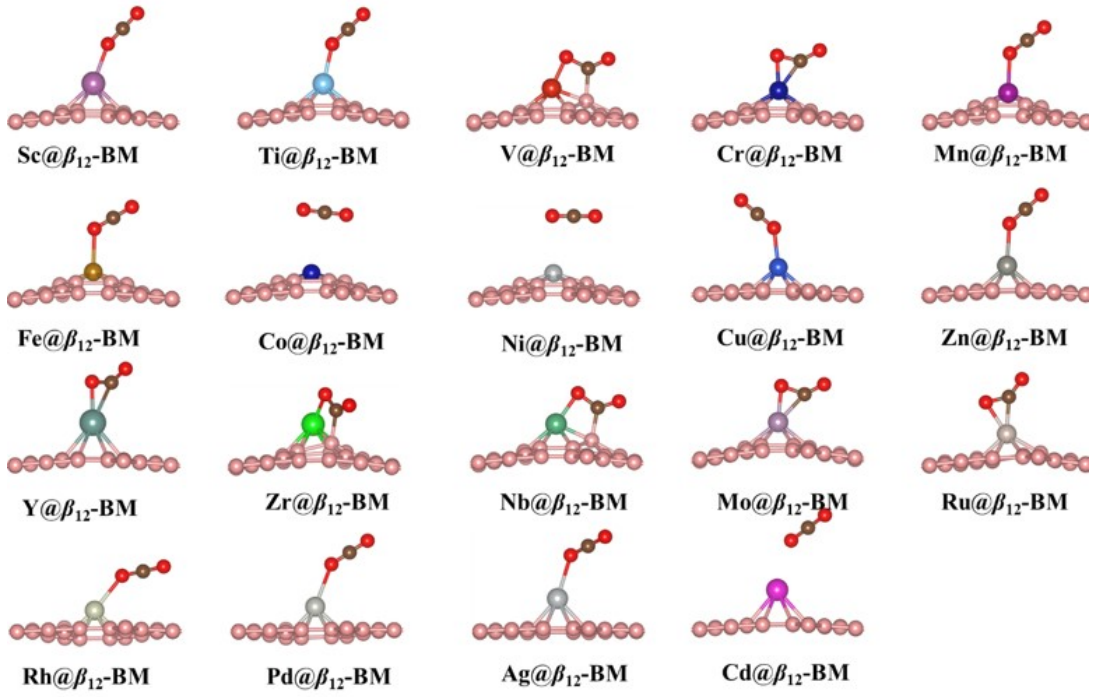

Figure S7. The optimized configuration of CO_2 adsorption on 19 catalysts (Model 1).

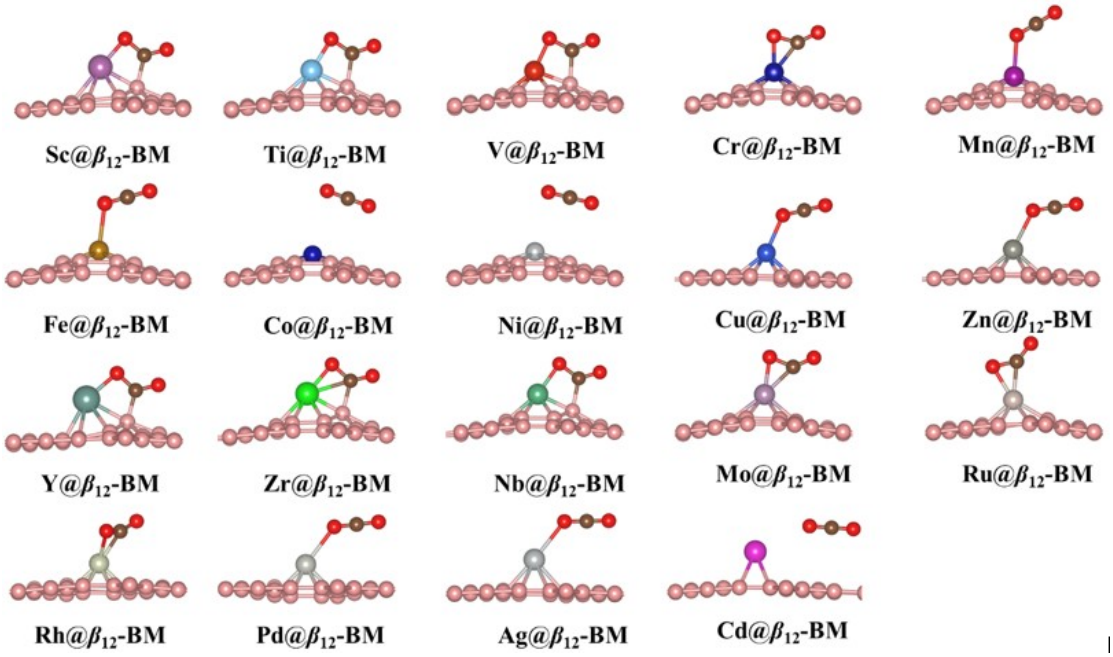

Figure S8. The optimized configuration of CO_2 adsorption on 19 catalysts (Model 2).

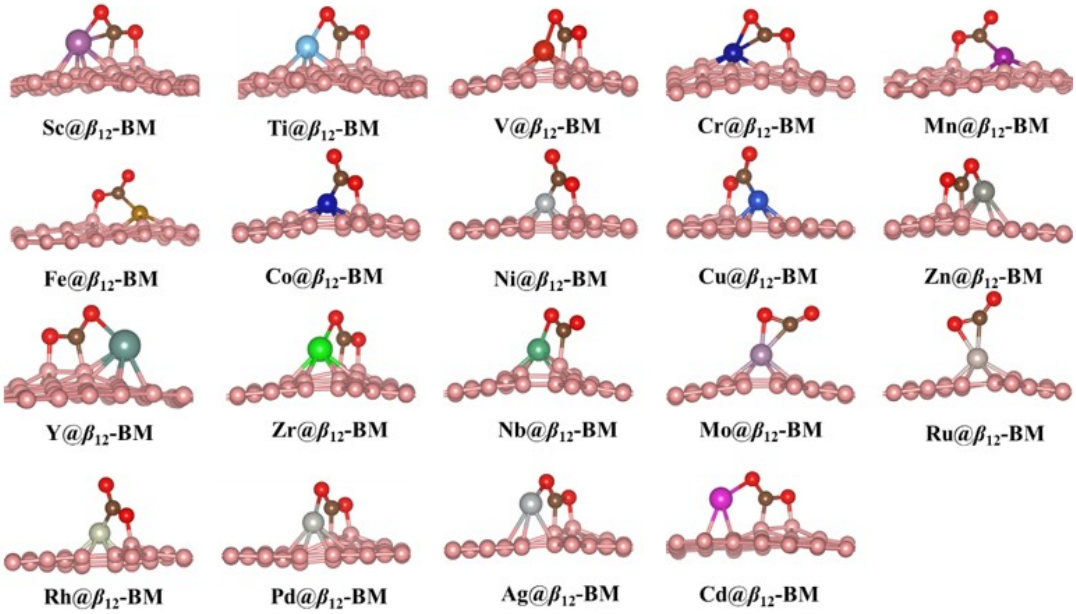

Figure S9. The optimized configuration of CO_2 adsorption on 19 catalysts (Model 3).

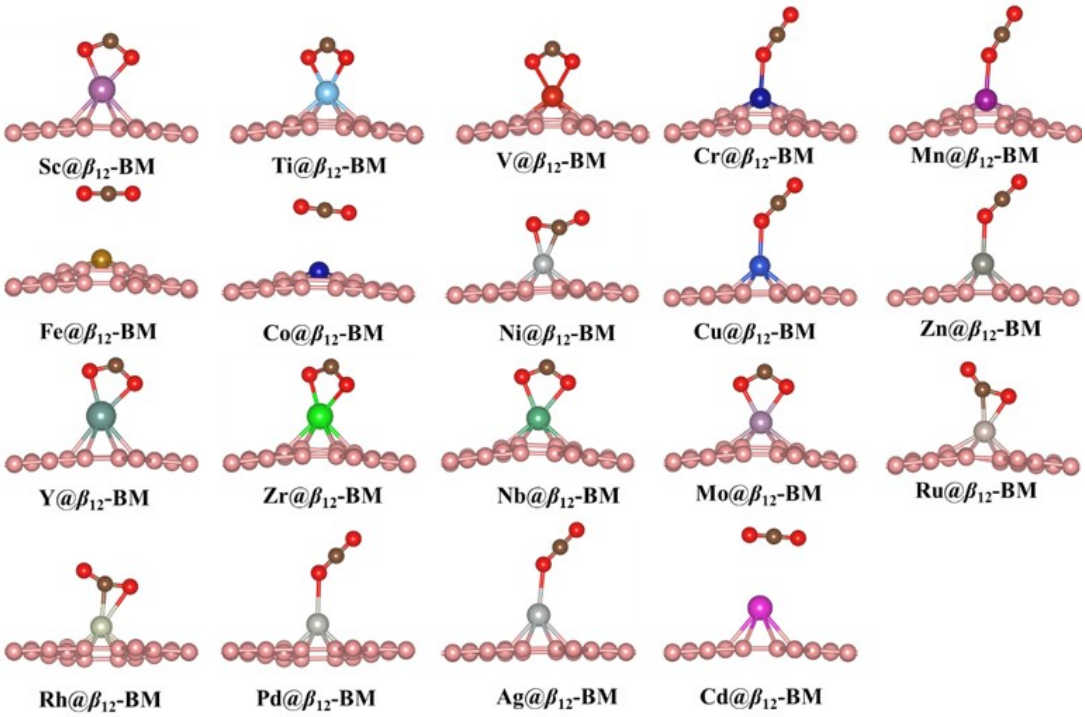

Figure S10. The optimized configuration of CO_2 adsorption on 19 catalysts (Model 4).

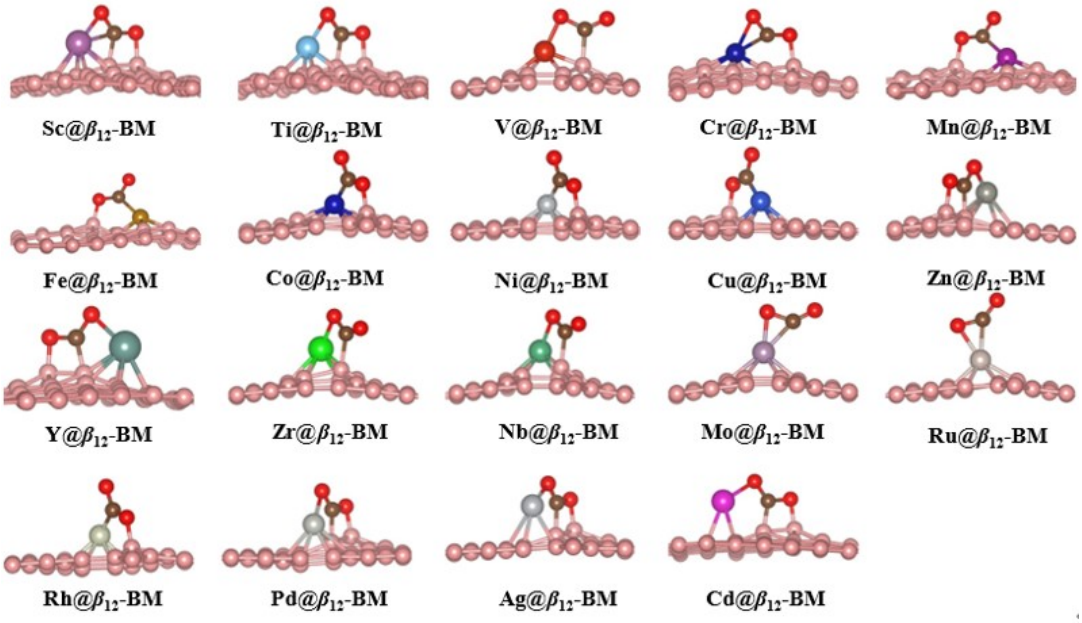

Figure S11. The most stable adsorption configuration of the selected CO_2 on each catalyst.

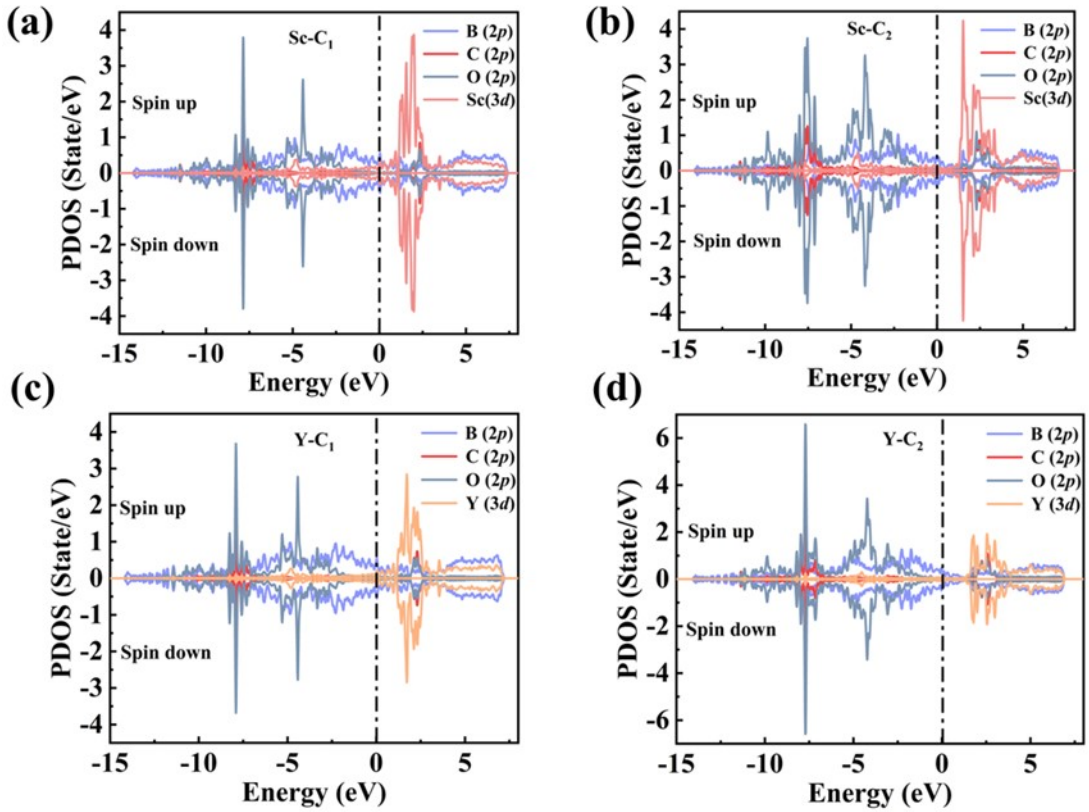

Figure S12. (a)–(d) the projected density of state (PDOS) of single CO_2 and two CO_2 molecules adsorption on the Sc@β_{12}-BM and Y@β_{12}-BM in the gas phase, respectively.

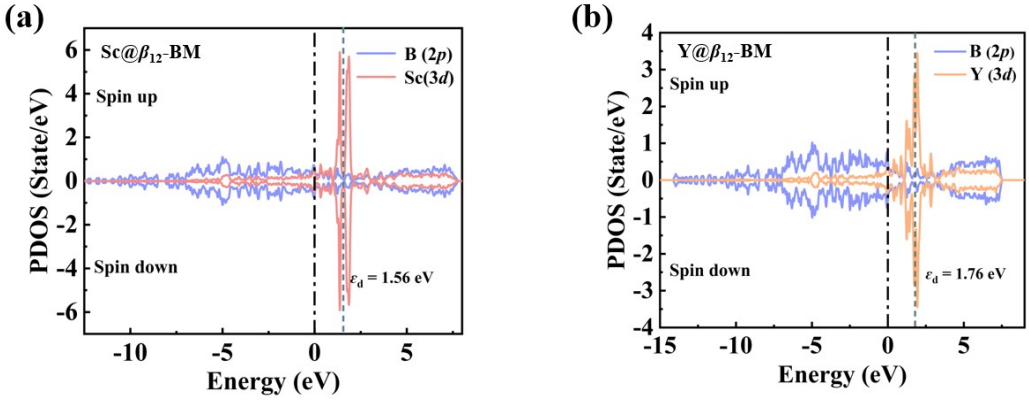

Figure S13. the projected density of state (PDOS) of Sc@β_{12}-BM and Y@β_{12}-BM, respectively.

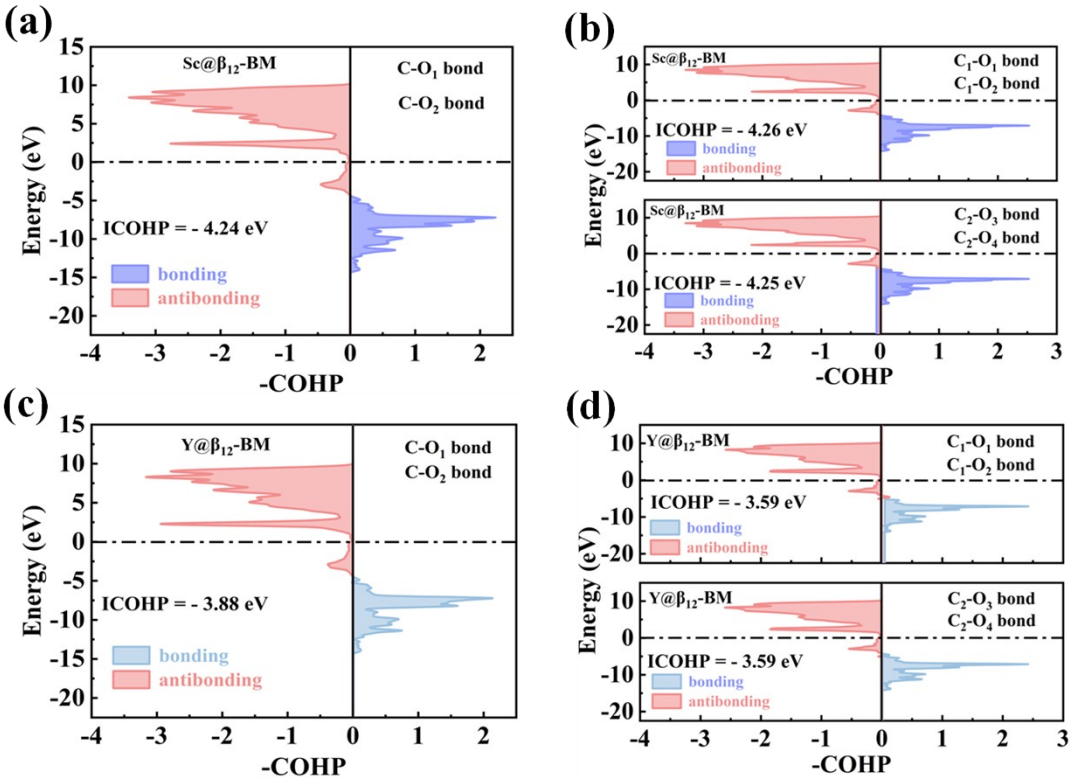

Figure S14. (a)–(d) projected crystal orbital Hamilton population (pCOHP) of single CO_2 and two CO_2 molecules adsorption on the Sc@β_{12}-BM and Y@β_{12}-BM in the gas phase, respectively.

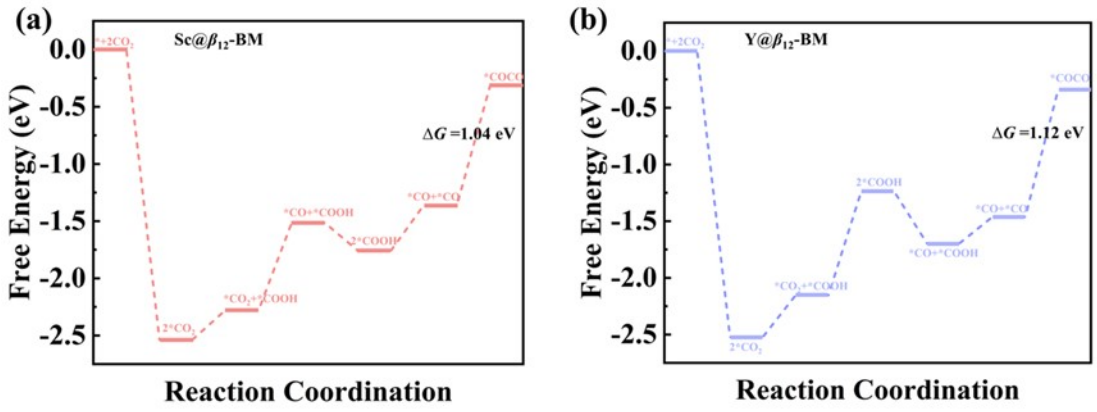

Figure S15. Gibbs free energy barrier diagram for the generation of *COCO on the (a) Sc@β_{12}-BM and (b) Y@β_{12}-BM, respectively.

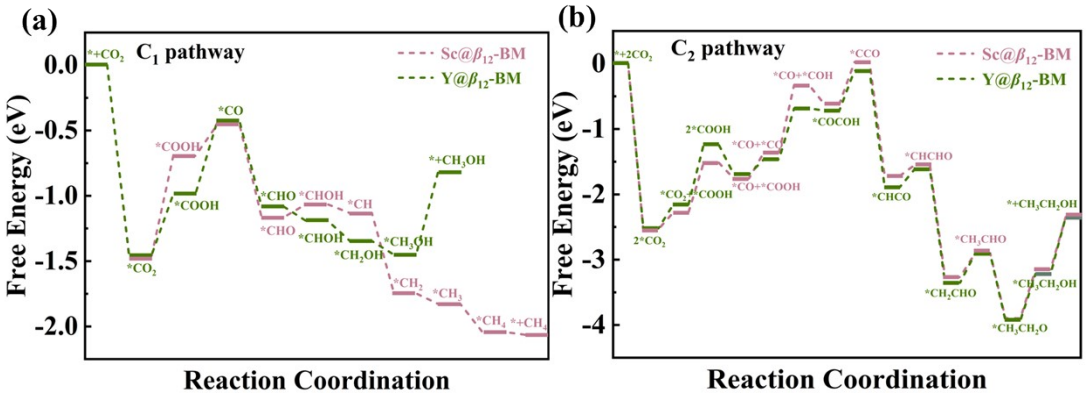

Figure S16. Free energy diagrams of CO_2RR through the most favorable C_1 and C_2 pathway on Sc@β_{12}-BM and Y@β_{12}-BM, respectively.

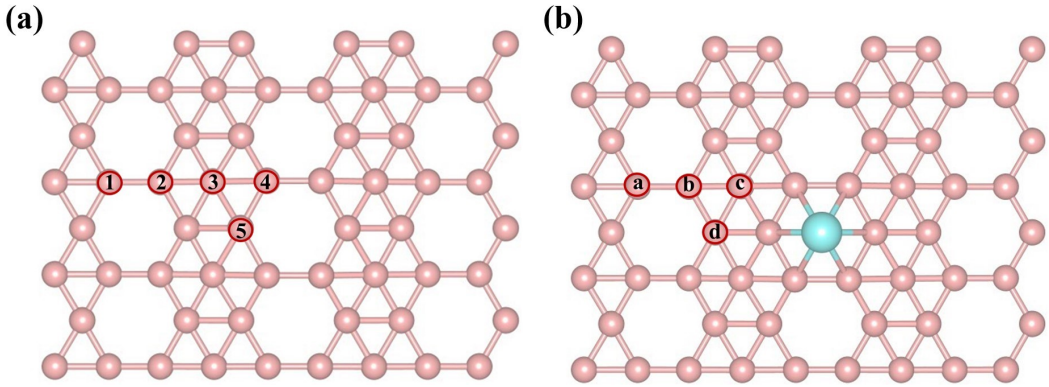

Figure S17. The CO_2 adsorption site on (a) original β_{12}-borophene and (b) TM@β_{12}-BM.

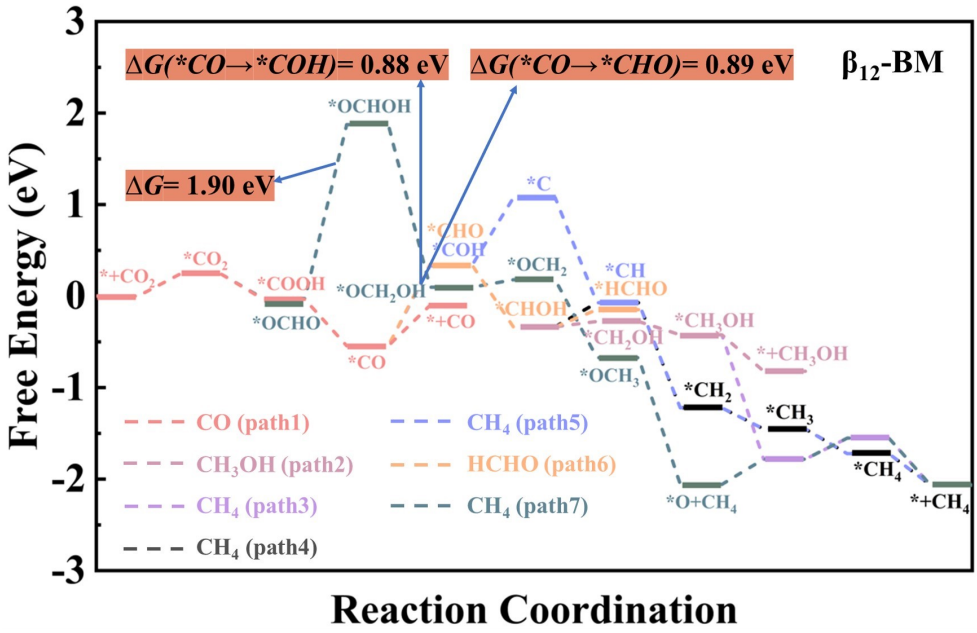

Figure S18. (a) Free energy diagram of the CO_2RR pathways to C_1 products on original β_{12}-borophene.

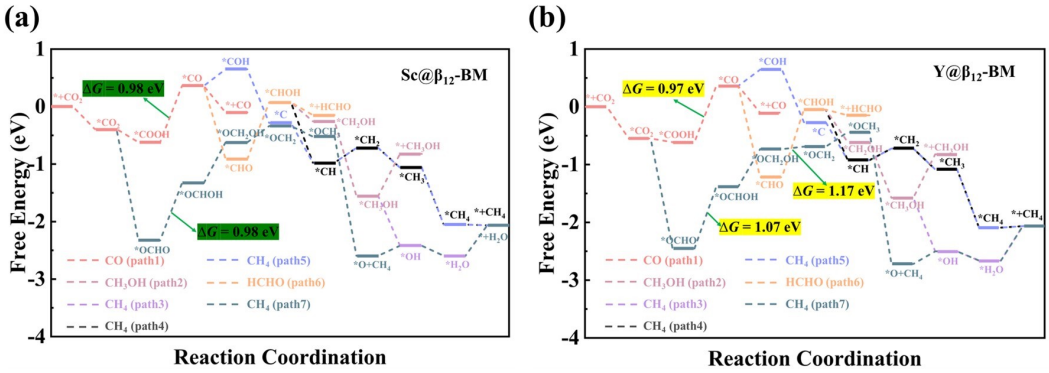

Figure S19. Free energy diagram of the CO_2RR pathways to C_1 products on pure B site of (a)Sc@β_{12}-BM and (b) Y@β_{12}-BM.

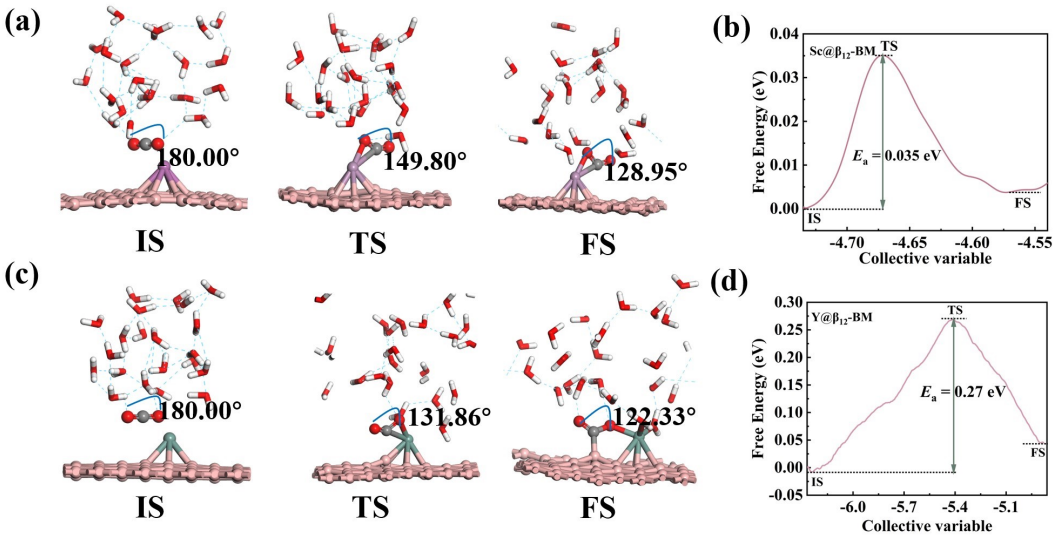

Figure S20. Structures of the initial, transition and final states of (a) and (c) CO_2 adsorption process on Sc@β_{12}-BM and Y@β_{12}-BM. (b) and (d) Free energy distribution of CO_2 adsorption process on Sc@β_{12}-BM and Y@β_{12}-BM in the liquid phase, respectively.

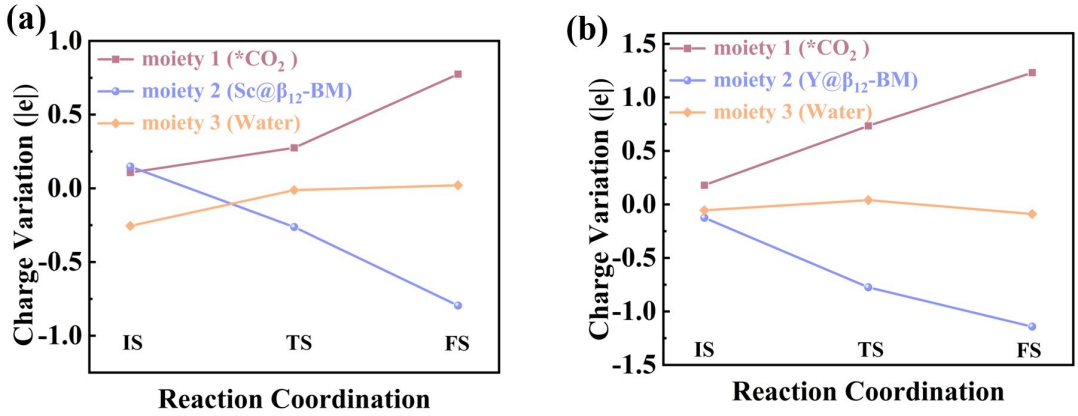

Figure S21. (a)−(b) Charge variation of the three moieties along two steps of C-C coupling reactions. Moieties 1, 2, and 3 represent the adsorbed CO_2, the Sc@β_{12}-BM and Y@β_{12}-BM, and the water molecules, respectively. The positive values represent the electron obtained; negative values represent the loss of electrons.

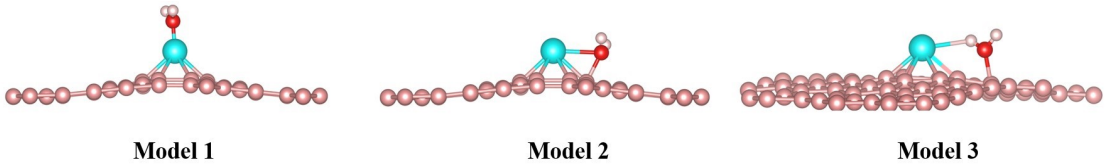

Figure S22. Initial adsorption configuration of H_2O on the Sc@β_{12}-BM and Y@β_{12}-BM.

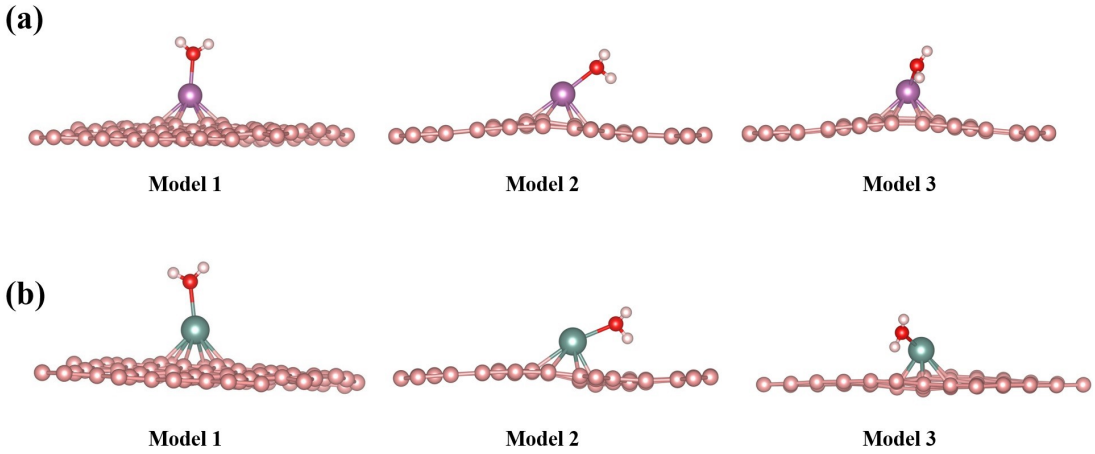

Figure S23. The optimized adsorption structure of H_2O on the (a) Sc@β_{12}-BM and (b) Y@β_{12}-BM.

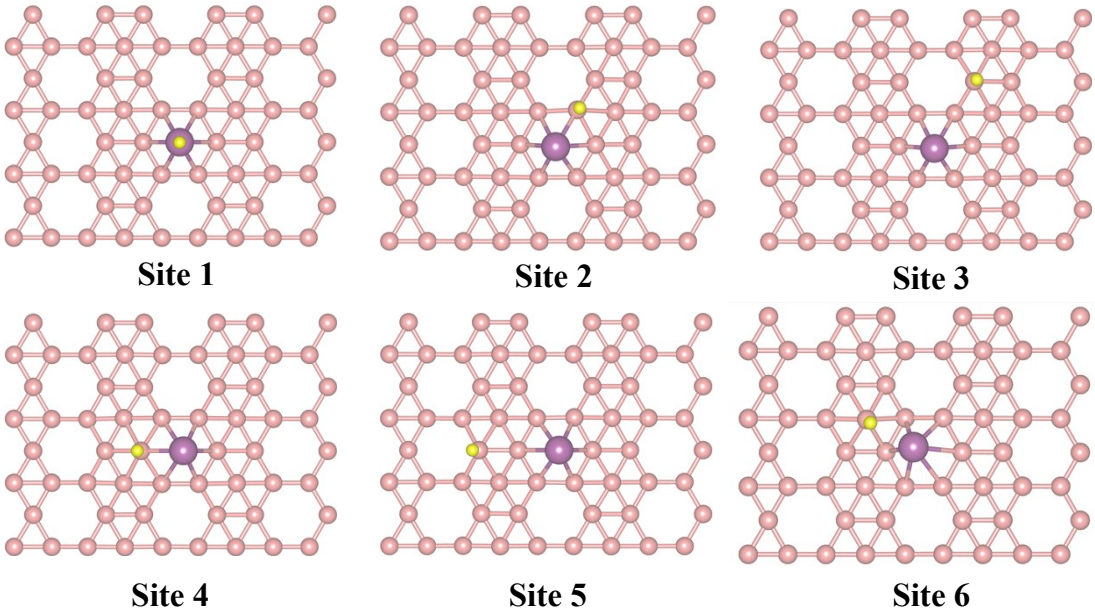

Figure S24. Optimized *H stable structure at six sites of Sc@β_{12}-BM.

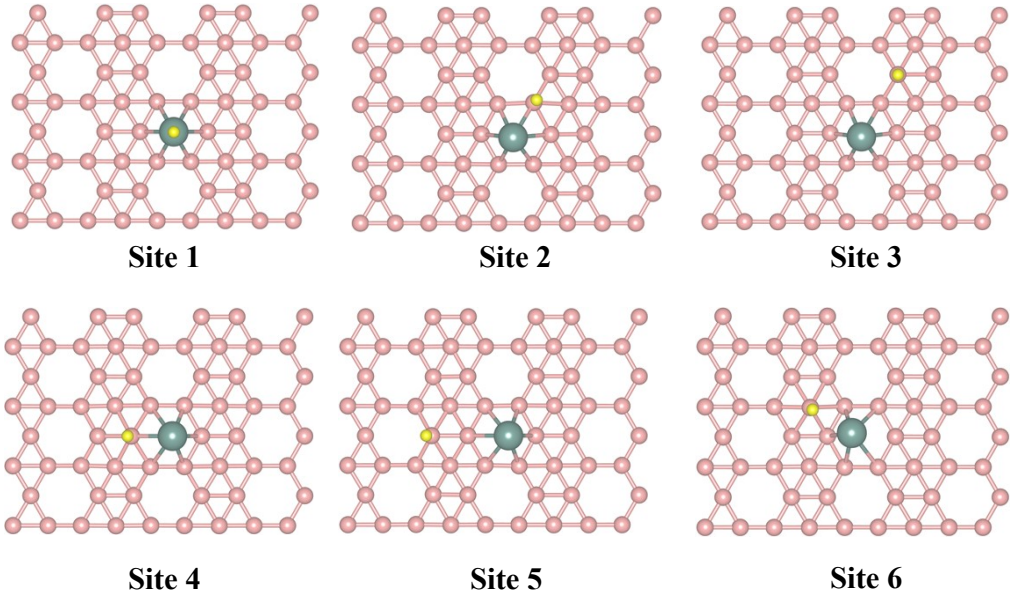

Figure S25. Optimized *H stable structure at six sites of Y@β_{12}-BM.

Table S1. Bond angle variation of CO_2 adsorbed by four different models of 3*d* and 4*d* transition metal doped β_{12}-BM ("–" represents the inability to absorb CO_2).

CO_2 angle(°)	Model 1	Model 2	Model 3	Model 4
Sc@β_{12}-BM	–	125.53	125.74	122.79
Ti@β_{12}-BM	–	127.20	127.71	123.84
V@β_{12}-BM	126.88	126.86	129.25	121.71
Cr@β_{12}-BM	138.50	138.78	130.94	–
Mn@β_{12}-BM	–	–	132.28	–
Fe@β_{12}-BM	–	–	129.56	–
Co@β_{12}-BM	–	–	126.88	–
Ni@β_{12}-BM	–	–	127.15	149.55
Cu@β_{12}-BM	–	–	127.29	–
Zn@β_{12}-BM	–	–	124.58	–
Y@β_{12}-BM	139.89	124.12	124.26	123.93
Zr@β_{12}-BM	126.68	126.14	126.35	120.17
Nb@β_{12}-BM	126.92	126.88	128.16	122.69
Mo@β_{12}-BM	133.25	133.57	128.64	117.47
Ru@β_{12}-BM	140.56	140.24	131.48	140.57
Rh@β_{12}-BM	–	148.20	125.42	153.76
Pd@β_{12}-BM	–	–	125.05	–
Ag@β_{12}-BM	–	–	123.72	–
Cd@β_{12}-BM	–	–	122.65	–

Table S2. Adsorption energy of CO_2 by 3*d* and 4*d* transition metal doped β_{12}-BM ("–" represents the inability to absorb CO_2).

.

E_{ads}(eV)	Model 1	Model 2	Model 3	Model 4
Sc@β_{12}-BM	–	-1.41	-1.78	-0.51
Ti@β_{12}-BM	–	-1.40	-1.56	-0.35
V@β_{12}-BM	-1.41	-1.41	-1.25	-0.16
Cr@β_{12}-BM	-0.98	-0.98	-0.65	–
Mn@β_{12}-BM	–	–	-0.40	–
Fe@β_{12}-BM	–	–	-0.17	–
Co@β_{12}-BM	–	–	-0.12	–
Ni@β_{12}-BM	–	–	-0.51	-0.29
Cu@β_{12}-BM	–	–	-0.29	–
Zn@β_{12}-BM	–	–	-0.73	–
Y@β_{12}-BM	-0.64	-1.36	-1.76	-0.61
Zr@β_{12}-BM	-1.37	-1.33	-1.53	-0.54
Nb@β_{12}-BM	-1.40	-1.40	-1.22	-0.47
Mo@β_{12}-BM	-1.03	-1.41	-0.82	-0.38
Ru@β_{12}-BM	-0.76	-1.14	-1.07	-1.14
Rh@β_{12}-BM	–	-0.63	-1.04	-0.67
Pd@β_{12}-BM	–	–	-0.13	–
Ag@β_{12}-BM	–	–	-0.61	–
Cd@β_{12}-BM	–	–	-0.73	–

Table S3. The adsorption energy of the adsorbed single CO_2 and two CO_2 molecules (E_{ads}), the angle of adsorbed CO_2 (degree), the bond length of adsorbed CO_2 (Å), number of electrons transferred from the catalyst to the CO_2 molecule (Δq) and crystal integral Hamiltonian population (ICOHP) in the gas phase for Sc@β_{12}-BM and Y@β_{12}-BM.

	Sc@β_{12}-BM					**Y@β_{12}-BM**				
	E_{ads} (eV)	Angle of CO_2 (degree)	Bond length of C–O (Å)	Δq (|e|)	ICOHP (eV)	E_{ads} (eV)	Angle of CO_2 (degree)	Bond length of C–O (Å)	Δq (|e|)	ICOHP (eV)
***CO_2**	–1.78	125.73	1.30	1.88	–4.24	1.76	124.26	1.28	1.39	–3.88
			1.27					1.30		
***2CO_2**	–3.16	125.00	1.27/1.30	1.27	–4.26	–3.13	123.44	1.28/1.30	1.38	–3.59
		124.98	1.30/1.27	1.31	–4.25		123.48	1.30/1.28	1.38	–3.59

Table S4. Adsorption free energies and bond angles of optimized CO_2 on pure β_{12}-borophene.

Model (β_{12}-BM)	**ΔG(*CO_2) (eV)**	**Bond Angle of CO_2 (°)**
1	0.17	127.22
2	–	180.00
3	–	180.00
4	0.24	122.28
5	–	180.00

Table S5. Adsorption free energies and bond angles of optimized CO_2 on pure B sites of TM@β_{12}-BM(TM = Sc, Y).

Model	Sc@β_{12}-BM		Y@β_{12}-BM	
	ΔG(*CO_2) (eV)	**Bond Angle of CO_2 (°)**	**ΔG(*CO_2) (eV)**	**Bond Angle of CO_2 (°)**
a	-0.66	124.94	-1.06	124.10
b	–	180	–	180
c	-0.39	117.72	-0.55	117.16
d	-0.87	121.62	-0.89	120.63

Table S6. Free energies of water adsorption at different sites on Sc@β_{12}-BM and Y@β_{12}-BM.

Sc@β_{12}-BM		**Y@β_{12}-BM**	
Model	**ΔG(*H_2O) (eV)**	**Model**	**ΔG(*H_2O) (eV)**
1	-0.55	**1**	-0.38
2	-0.52	**2**	-0.61
3	-0.59	**3**	-0.67